[UO2(NH3)5]Br2 · NH3: Synthesis, Crystal Structure, and Speciation in Liquid Ammonia Solution by First-Principles Molecular Dynamics Simulations.†

Patrick Woidy,[a] Michael Bühl,[b,*] and Florian Kraus[c,*]

Pentaammine dioxido uranium(VI) dibromide ammonia (1/1), $[UO_2(NH_3)_5]Br_2 \cdot NH_3$, was synthesized in the form of yellow crystals by the reaction of uranyl bromide, UO_2Br_2, with dry
10 liquid ammonia. The compound crystallizes orthorhombic in space group *Cmcm* and is isotypic to $[UO_2(NH_3)_5]Cl_2 \cdot NH_3$ with $a = 13.2499(2)$, $b = 10.5536(1)$, $c = 8.9126(1)$ Å, $V = 1246.29(3)$ Å^3 and $Z = 4$ at 123 K. The UO_2^{2+} cation is coordinated by five ammine ligands and the coordination polyhedron can be best described as pentagonal bipyramid. Car-Parrinello molecular dynamics simulations are reported for $[UO_2(NH_3)_5]^{2+}$ in the gas phase and in liquid NH_3 solution (using the
15 BLYP density functional). According to free-energy simulations, solvation by ammonia has only a small effect on the uranyl-NH_3 bond strength.

1 Introduction

Fueled by continued industrial use and driven by advances in
20 synthetic techniques, uranium chemistry has been blossoming of late.[1] One of the key elements in this development is the move from water to organic solvents, which has given access to a plethora of new uranium compounds with unusual oxidation states and new bonding motifs. However, one
25 solvent that is quite common in inorganic synthesis has received relatively little attention so far in uranium chemistry, namely liquid ammonia. We have explored its use for preparative purposes and have added a number of uranium-ammonia compounds to the growing portfolio of uranyl(VI)
30 and uranium(IV) complexes.[2,3] We now report on a new compound that was isolated during our speciation studies, $[UO_2(NH_3)_5]Br_2 \cdot NH_3$.

Liquid anhydrous ammonia is widely used in industry, mainly
35 for refrigeration purposes. It has some attractive properties for use as a solvent, such as the possibility to work at low temperatures. Its polarity is between that of water, the traditional medium for uranyl(VI) chemistry, and that of inert organic solvents, which have led to the "renaissance" of
40 uranium chemistry. It is thus conceivable that working in liquid ammonia can open up new avenues in uranium chemistry.

To understand the chemistry of uranium compounds in
45 ammonia at an atomistic level and to help design new species and processes, e.g. for selective complexation and separation, first-principles modelling will be instrumental. For actinoid compounds in general, and uranyl complexes in particular, ab initio and density functional theory (DFT) calculations have a
50 long history and are now well established.[4] The vast majority of these studies attempt to model an aqueous environment, either by way of static optimisations and implicit solvation through polarisable continuum models (PCMs), or by explicit inclusion of the solvent in a dynamic ensemble. In the latter
55 spirit, we have been using Car-Parrinello molecular dynamics (CPMD) simulations to model a number of uranyl complexes in aqueous solution.[5,6,7] Using this method, together with a special numerical technique (pointwise thermodynamic integration, PTI), several thermodynamic and kinetic
60 parameters of uranyl hydrate, $[UO_2(H_2O)_5]^{2+}$, have been reproduced with an accuracy of ca. ±2.5 kcal/mol. We have also reported the first CPMD simulations of uranyl complexes in a non-aqueous solvent (acetonitrile).[8] We now apply this approach to the prototypical uranyl complex in ammonia,
65 $[UO_2(NH_3)_5]^{2+}$. Special attention is called to the effect of the ammonia medium on the uranyl-NH_3 bond strength, as compared to that of an aqueous environment on the corresponding uranyl-water affinity in uranyl hydrate.

2 Experimental and Computational details

70 All experiments were carried out excluding humidity and air in an atmosphere of dried and purified argon (Westfalen AG) using a high-vacuum glass line or a glove box (MBraun). Liquid ammonia (Westfalen AG) was dried and stored over sodium (VWR) in a special high-vacuum glass line. All
75 vessels used for reactions with liquid ammonia were made of borosilicate glass and flame-dried before use.

Synthesis and crystallization
UBr_4 was oxidized in anhydrous ammonia by bubbling O_2

through the solution which leads to formation of dissolved and solvated UO_2Br_2 besides Br_2 at -78 °C. The latter oxidizes ammonia under formation of N_2 and NH_4Br. Pure, anhydrous UO_2Br_2 was obtained by evaporation of the solvent at -34 °C
5 and further heating to approximately 100 °C under a high vacuum (ca. 10^{-6} mbar) where further NH_3 and the NH_4Br are pumped off. 0.25 g (0.58 mmol) UO_2Br_2 were placed in a reaction flask under argon atmosphere. After cooling to −78 °C approximately 10 mL liquid ammonia were condensed on
10 top of the red powder of UO_2Br_2 resulting in a clear yellow solution and a solid residue. Yellow single crystals of the title compound were obtained from storage at −40 °C after ten days. A suitable single crystal was selected under perfluoroether oil using the MiteGen system. As the
15 compound is an ammoniate it is unstable upon warming above approximately -30 °C. The crystals burst due to the rising ammonia vapour pressure. Further analysis of the compound can therefore not be undertaken.

20 *Structure Solution and Refinement*
The structure was solved by using Direct Methods implemented in Shelxs and refined on F^2 using Shelxl.[9] The atoms (except for the hydrogen atoms) were located from the difference Fourier map. All atoms were refined
25 anisotropically. The hydrogen atoms were added by using a riding model. The crystal structure does not show any features where special refinement procedures had to be applied. The residual electron densities are close to the uranium atom.
CPMD Simulations
30 Initial simulations were performed for a solution of $[UO_2(NH_3)_5]^{2+}$ in liquid NH_3. To facilitate comparison with previous work on aqueous uranyl,[5] essentially the same methodology was used, namely CPMD[10] / BLYP[11] simulations using Troullier-Martins pseudopotentials,[12] periodic boundary
35 conditions with a plane-wave basis set (80 Ry cut-off), a fictitious electronic mass of 600 a.u., a time step of 0.121 fs and the mass of D instead of H.[13] The complex was immersed in a cubic box with box size of 13.22 Å filled with 37 NH_3 molecules, corresponding to a density of 0.71 (this value was
40 arrived at by taking the number of solvent water molecules in our previous simulation of aqueous UO_2^{2+} [11] and scaling the density of the solvent from 1.0 to 0.61, the density of liquid NH_3 at 20°C). The starting structure was built from a well-equilibrated solution of $[UO_2(H_2O)_5]^{2+}$ in water, changing O
45 to N, deleting the appropriate number of solvent molecules and adding the missing H atoms. The system was first equilibrated in the NVE ensemble for 2 ps maintaining a temperature of 273 ± 50 K using velocity rescaling, then propagated freely for another 7 ps, at the end of which the
50 temperature had equilibrated to 283 ± 13 K. Analogous simulations have been performed for in $[UO_2(NH_3)_5]^{2+}$ in the gas phase, starting from the fully optimised minimum (the latter denoted CP-opt); this simulations have been run for 3 ps, after which the temperature has equilibrated to 317 ± 41
55 K. For the free-energy PTI simulations the distance r between U and one N atom of a bound ammonia ligand was taken as reaction coordinate[14] and elongated in steps of 0.2 Å until the

resulting free-energy profile levelled off (see Supporting Information for further details). These computations were
60 performed with the CPMD program.[15]

The BLYP functional was chosen because of its good performance for the properties of liquid NH_3.[12] Because the simulations were performed at constant volume, Helmholtz
65 rather than Gibbs free energies are obtained, but in condensed phase the difference between both is very small. No further dissection of the free energies into enthalpic and entropic contributions (which would require, in principle, simulations at different temperatures) was attempted.

70
Selected nonperiodic geometry optimisations were performed at BLYP, and B3LYP[16,10b] levels, employing the small-core Stuttgart-Dresden relativistic ECP together with its valence basis set on U[17] (from which the most diffuse s-,p-,d-, and f-
75 functions were omitted, affording a [7s6p5d3f] contraction),[18] standard 6-311G+(d,p) basis[19] for all other elements, and an ultrafine integration grid (99 radial shells with 590 angular points per shell), denoted SDD. The minimum character of each stationary point was verified by computation of the
80 harmonic vibrational frequencies, which were all real. Selected structures were reoptimised in a polarisable continuum (IEF-PCM,[20] see supporting information for details and references) and subject to natural population and natural bond orbital analysis.[21] These computations were performed
85 with the Gaussian suite of programs.[22]

3 Results and discussion

3.1 Structures

Yellow crystals of pentaamine dioxido uranium(VI)
90 dibromide ammonia (1/1), $[UO_2(NH_3)_5]Br_2 \cdot NH_3$, were prepared from the reaction of UO_2Br_2 with dry liquid ammonia according to equation 1.

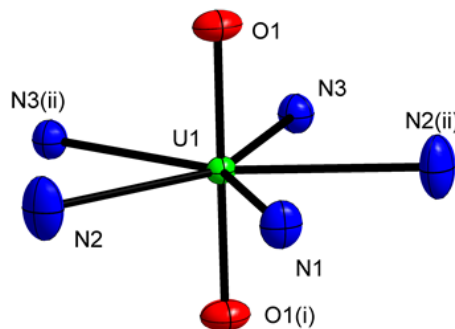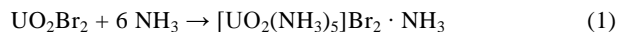$$UO_2Br_2 + 6\ NH_3 \rightarrow [UO_2(NH_3)_5]Br_2 \cdot NH_3 \qquad (1)$$

95

Figure 1: The pentaammine dioxido uranium(VI) dication of the title compound. Displacement ellipsoids are shown at the 70 % probability level at 123 K, H atoms omitted. [Symmetry codes: (i) x, y, $-z + 1/2$;
100 (ii) $-x + 1$, y, $-z + 1/2$.].

The title compound crystallizes in the orthorhombic space group *Cmcm* (No. 63) isotypic to the previously reported $[UO_2(NH_3)_5]Cl_2 \cdot NH_3$.[2] The uranium atom occupies the 4*c* position, and the oxygen atom O1 the 8*f* position forming with
[5] its symmetry equivalent the uranyl cation. The $[UO_2]^{2+}$ cation is coordinated by five ammine ligands (N1, N2 and N3 and their symmetry equivalents). A projection of the discrete pentaammine dioxido uranium(VI) cation, $[UO_2(NH_3)_5]^{2+}$, is shown in Figure 1. The ammonia molecule of crystallization
[10] occupies the 4*c* and the bromide anion the 8*e* position. The U−O distance of the almost linear uranyl cation (O−U−O angle of 179.1(2)°) is 1.771(3)Å. Comparable distances were reported for the alkali metal uranyl nitrates $M[UO_2(NO_3)_3]$ with *M*= K,[23,24] Rb,[25,26] and Cs[27] of 1.746 to 1.795Å. The U−N
[15] distances of the title compound are observed in a range from 2.522(3) to 2.577(3) Å. The U−N distances of the isotypic compound $[UO_2(NH_3)_5]Cl_2 \cdot NH_3$ (2.505(2) to 2.554(3) Å) or the compound $[UO_2F_2(NH_3)_3]_2 \cdot 2 NH_3$ (2.526(4) to 2.567(3) Å) differ only slightly from the U−N distances reported here.[2]
[20] In $[UF_4(NH_3)_4] \cdot NH_3$ longer U−N distances of 2.618(5) Å were reported due to the higher coordination number.[3] The closest U-Br distances are observed with 4.9480(3) Å, which is marginally shorther compared to the isotypic chloride (4.9554(3) Å). The compound shows N-H…Br and N-H…N
[25] hydrogen bonding, but caution is advised for its discussion as the N atoms reside on special positions (N(1) on *m2m*, N(2, 3) on *..m*). Therefore only the H atoms on N(2) and N(3) could be located properly. The hydrogen atoms bound to the N(2) atom form N-H…Br hydrogen with H…Br distances in the
[30] range of 2.67 to 2.99 Å, and N-H…Br angles from 124.5 to 172.3°. The H atoms on N(3) form two N-H…Br hydrogen bonds with H…Br distances of 2.59 and 2.76 Å, and angles of 177.0 and 139.4°, respectively. The third H atom on N(3) forms a N-H…N hydrogen bond with a H…N distance of 2.24
[35] Å and an N-H…N angle of 159.2°. These hydrogen bond parameters are comparable to the ones previously reported.[2] The unit cell of the title compound $[UO_2(NH_3)_5]Br_2 \cdot NH_3$ is shown in Figure 2, crystallographic details are available from Table 1.
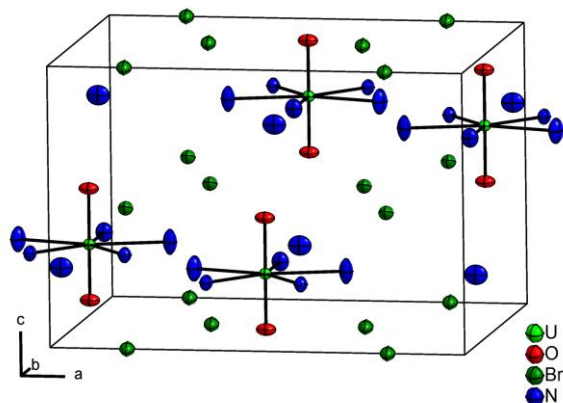

[40]
Figure 2: The unit cell of the title compound. Displacement ellipsoids are shown at the 70 % probability level at 123 K, H atoms

omitted.

[45] **Table 1.** Crystallographic details of the title compound. Further details of the crystal structure investigation are available from the Fachinformationszentrum Karlsruhe, D-76344 Eggenstein−Leopoldshafen (Germany), http://www.fiz-karlsruhe.de/icsd.html, on quoting the depository number
[50] CSD- 429046.

	Title Compound
Formula	$H_{18}Br_2N_6O_2U$
Color	yellow
Habitus	block
Size [mm³]	0.15 x 0.3 x 0.35
M_r [g mol⁻¹]	531.91
Crystal system	orthorhombic
Space group	*Cmcm* (No. 63)
a [Å]	13.2499(2)
b [Å]	10.5536(1)
c [Å]	8.9126(1)
V [Å³]	1246.29(3)
Z	4
ρ_{calc} [g m⁻³]	2.80
λ [Å]	0.71073
T [K]	123(2)
$\mu(Mo_{K\alpha})$ [mm⁻¹]	19.42
R_{int}	0.039
R(F) (*I*≥2*σ(I)*, all data)	0.023, 0.025
wR(F²) (*I*≥2*σ(I)*, all data)	0.059, 0.060
S (all data)	1.13
Data, parameters, restraints	1949, 40, 1
$\Delta\rho_{max}$, $\Delta\rho_{min}$ [e Å⁻³]	4.21, −2.90

Subsequently we studied the pristine $[UO_2(NH_3)_5]^{2+}$ cation of the title compound computationally. The observed five-coordination mode remained stable in vacuo and in ammonia
[55] solution (i.e. no spontaneous dissociation or association of ligands occurred). The resulting structural parameters are collected in Table 2.

Table 2. Optimised or mean simulated bond distances in
[60] $[UO_2(NH_3)_5]^{2+}$ (in Å).

Level[a]	U=O[b]	U-N[b]
CP-opt(g)	1.783	2.667
BLYP(g)	1.788	2.661
BLYP(PCM)	1.801	2.619
B3LYP(g)	1.754	2.634
B3LYP(PCM)	1.765	2.596
CPMD(g)	1.79(2)	2.69(10)
CPMD(l)	1.81(3)	2.62(9)
X-Ray[c]	*1.771(3)*	*2.536(3)*

[a]CPMD: mean values during 2 ps of unconstrained MD (BLYP level, standard deviation in parentheses) in the gas phase (g) or liquid ammonia solution (l); BLYP, B3LYP: optimised parameters using the respective functional (SDD/6-
[65] 311+G**basis) in the gas phase (g) or a polarisable continuum (PCM). [b]Mean values. [c]This work.

On going from the gas phase into solution, the U-N distance is computed to decrease notably, by ca. -7 pm (compare CPMD(g) and CPMD(l) values in Table 2). A similar decrease (-6 pm) had been observed for the U-O(water) bond in the pentahydrate upon solvation.[12] A slightly smaller, but still notable contraction of ca. -4 pm is obtained upon immersion in a polarisable continuum (compare BLYP(g) and BLYP(PCM) values in Table 2). The simulated mean U-N distance in solution, 2.62 Å, is notably elongated compared to that found experimentally in the title compound in the solid[28] (2.522(3) to 2.577(3) Å). It is likely that the BLYP functional employed in the CPMD simulations (which is used for its good description of liquid water and NH_3)[13] inherently overestimates this distance, as frequently found for metal-ligand distances in general.[29] A slight decrease is found on going to a hybrid functional (compare BLYP(g) and B3LYP(g), or BLYP(PCM) and B3LYP(PCM) data in Table2), but using this in the MD simulations would be too expensive.

The structure of $[UO_2(NH_3)_5]^{2+}$ in liquid NH_3 was further characterised in terms of the U-N pair correlation (or radial distribution) function displayed in Figure 3. The width of the first maximum between 2.4 and 3.0 Å illustrates the soft binding mode of the ammonia ligands, which is also reflected in the large standard deviations of the averaged distances in Table 1 (numbers in parentheses).
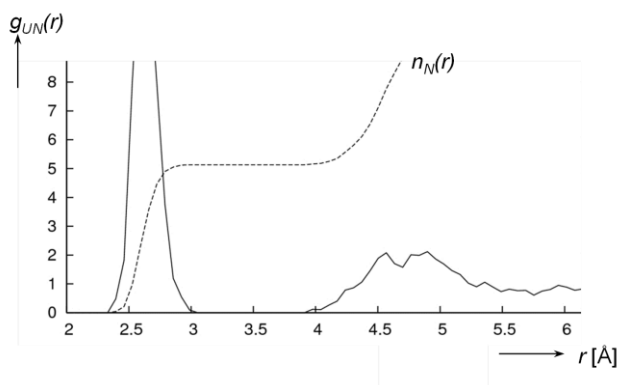

Figure 3: U-N pair correlation function for $[UO_2(NH_3)_5]^{2+}$ in liquid NH_3 (dashed: integrated to give the mean number of N atoms around U at a given distance r; data collected during the last 5 ps of simulation).

There is clear indication of a second solvation shell, manifest in a broad maximum of the U-N pair correlation function between ca. 4 Å and 5.5 Å (maximum value $g_{UN} \approx 2.1$). Integration of the pair correlation function between 3.9 Å and 5.75 Å (where g_{UN} assumes the lowest value in this area) affords a mean number of 12 ammonia molecules within this second solvation sphere.

3.2 Uranyl-NH_3 Bond Strength

In gaseous $[UO_2(H_2O)_5]^{2+}$ one water ligand is unbound at the BLYP level, i.e. a "4+1" structure with a water molecule H-bonded to $[UO_2(H_2O)_4]^{2+}$ in the second hydration shell is more stable (by -2.2 kcal/mol), and it is only in aqueous solution that the regular five-coordination is preferred (Figure 4a).[12] In contrast, all five ammonia ligands in $[UO_2(NH_3)_5]^{2+}$ are bound in the gas phase already. This is found in static geometry optimisations, where $[UO_2(NH_3)_4]^{2+}\cdot NH_3$ is higher in energy than $[UO_2(NH_3)_5]^{2+}$ (by ΔE = 6.4, 5.3, and 8.2 kcal/mol at the CP-opt, BLYP(g) and B3LYP(g) levels, respectively). The same is apparent upon tracing the free-energy pathway for NH_3 dissociation using constrained MD and thermodynamic integration, where the dissociation is endergonic (by ΔA = 5.3 kcal/mol, see the dotted pathway in Figure 4b).

That uranyl intrinsically (in the gas phase) binds NH_3 stronger than water is borne out by direct assessment via:

$$[UO_2(NH_3)_5]^{2+} + 5\ H_2O\ \rightarrow\ [UO_2(H_2O)_5]^{2+} + 5\ NH_3,$$
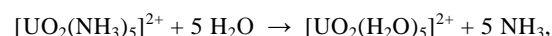
for which ΔE = +21.9 kcal/mol is computed at the BLYP (g) level [+20.9 kcal/mol at B3LYP(g)]. An even stronger intrinsic preference of N-donor ligands over water had been noted previously for acetonitrile.[30]

Solvation stabilises the five-coordinate ground state of $[UO_2(NH_3)_5]^{2+}$, so that the free energy of dissociation is increased to ΔA = 9.1 kcal/mol in liquid NH_3 (passing over a shallow barrier of $\Delta A^{\ddagger}$ = 10.9 kcal/mol). This finding is in line with the decrease of the mean U-N bond upon solvation discussed above.
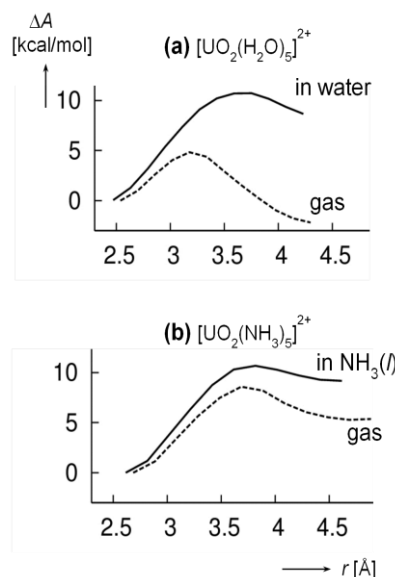

Figure 4: Helmholtz free energy profiles for dissociating one ligand L from $[UO_2L_5]^{2+}$ in the gas phase (dashed lines) and in solution (bold lines); top: L = H_2O, bottom: L = NH_3 (reaction coordinate r: U-O and U-N distance, respectively).

The absolute computed uranyl-ligand bond strengths in the respective solvents are thus indicated to be surprisingly

similar for water and ammonia (both ca. 9 kcal/mol). The relative solvation effects (with respect to the gas phase) are predicted to be quantitatively different, however: the higher coordination number is favoured in solution by ca. 11 kcal/mol and by ca. 4 kcal/mol for water and ammonia, respectively (compare Figure 4a and 4b). The apparent reduction of solvation effects on uranyl-ligand bond strengths in ammonia may be good news for continuum solvation models, because the accuracy of these models tends to deteriorate with increasing strength of specific solute-solvent interactions. Detailed performance studies of such PCM methods are beyond the scope of the present investigation, however.

According to natural population analysis, the bonding between U and N in $[UO_2(NH_3)_5]^{2+}$ is largely ionic, but with significant covalent character: the Wiberg bond index (WBI),[31] which approaches values close to 1 for fully covalent single bonds, is 0.44 between U and N (BLYP(PCM) level), and a natural bond orbital (NBO) analysis finds five localised U-N NBOs, which are however highly polarised toward N (12% contribution from U with comparable shares from s, p, d, and f orbitals). These bonds provide a means for charge transfer to the metal, as reflected in a natural charge of +0.69 for the UO_2 moiety, as opposed to +2 for bare $[UO_2]^{2+}$. The U-OH$_2$ bond in $[UO_2(H_2O)_5]^{2+}$ is computed to have a slightly higher ionic character (U-O WBI of 0.43 and natural charge of +0.81 on UO_2 at the same level).

The NH_3 dissociation in Figure 4b is a possible mechanism for ligand/solvent exchange in $[UO_2(NH_3)_5]^{2+}$; an alternative associative path via a six-coordinate intermediate or transition state needs to be studied (in analogy with the aquo complex, where such an associative interchange is preferred).[5,32]

4 Conclusions

In summary, we have structurally characterised a new member of the family of pentaammine uranyl complexes, $[UO_2(NH_3)_5]Br_2 \cdot NH_3$, which can be readily prepared in liquid ammonia. We have further characterised the structure of the pristine cation, $[UO_2(NH_3)_5]^{2+}$, in the same solvent through the first DFT/BLYP-based CPMD simulations of this system. According to free-energy simulations the uranyl-NH_3 bond strength in ammonia is similar to that of the uranyl-water bond in aqueous $[UO_2(H_2O)_5]^{2+}$, ca. 9 kcal/mol. However, the effect of the solvent on this property is markedly weaker for ammonia than for water. This effect is still noticeable in ammonia, though (reinforcement of the bond strength by 4 kcal/mol with respect to the gas phase). Thus, uranyl chemistry in this solvent may indeed be different from that in water or in truly inert organic solvents.

Our findings open up numerous opportunities for joint experimental and computational studies to explore and design new uranium chemistry. The renaissance of this chemistry may not be approaching its end just yet.

Notes and references

^{a} Technische Universität München, Zentrale Techn.-Wiss. Betriebseinheit, Radiochemie München, Walther-Meißner-Str. 3, 85747 Garching, Germany.
^{b} EaStCHEM School of Chemistry, North Haugh, University of St. Andrews, St. Andrews, Fife KY16 9ST, UK, E-mail: buehl@st-andrews.ac.uk
^{c} Anorganische Chemie, Fluorchemie, Philipps-Universität Marburg, Hans-Meerwein-Str. 4, 35032 Marburg, Germany, email: florian.kraus@chemie.uni-marburg.de.

† Electronic Supplementary Information (ESI) available: Additional computational details and references (including full citation for reference 19).. See DOI: 10.1039/xxxx/

1   For some selected reviews see e.g.: (a) P. L. Arnold, J. B. Love, D. Patel, *Coord. Chem. Rev*. 2009, **253**, 1973-1978; (b) S. Fortier, T. W. Hayton, *Coord. Chem. Rev*. 2010, **254**, 197-214; (c) K. E. Knope, L. Soderholm, *Chem. Rev*. 2013, **113**, 944–994; (d) M. Altmaier, X. Gaona, T. Fanghänel, *Chem. Rev*. 2013, **113**, 901–943; (e) Special edition of *Coord. Chem. Rev*. on "Recent Developments in the Chemistry of the Actinide (5f) Elements", B. Levason (Ed.), preface: B. Levason, *Coord. Chem. Rev*. 2014, **266-267**, 1.
2   P. Woidy, A. J. Karttunen, F. Kraus, *Z.Anorg.Allg.Chem.* 2012, **638**, 2044–2052.
3   F. Kraus, S. A. Baer, *Chem. Eur. J* **2009**, **15**, 8269–8274.
4   For some selected reviews see: (a) D. Wang, W. F. van Gunsteren, Z. Chai, *Coord. Chem. Rev.,* 2012, **41**, 5836-5865; (b) G. A. Shamov, *Acc. Chem. Res*., 2010, **43**, 19-29; (c) R. G. Denning, *J. Phys. Chem. A,* 2007, **111**, 4125-4143; (d) Z. Szabó, T. Toraishi, V. Vallet, I. Grenthe, *Coord. Chem. Rev.,* 2006, **250**, 784-815; (e) N. Kaltsoyannis, P. J. Hay, J. Li, J. P. Blaudeau, B. E. Bursten, in: *The Chemistry of the Actinide and Transactinide Elements*, 3rd ed.; Morss, L. R., Edelstein, N. M., Fuger, J., Katz, J. J., Eds.; Springer: Dordrecht, The Netherlands, 2006; Vol. 3, pp 1893-2012.
5   Review: M. Bühl, G. Wipff, *ChemPhysChem*, 2011, **12**, 3095-3105.
6   For more recent applications of this technique see e.g.: (a) M. Bühl, I. Grenthe, *Dalton Trans.*, 2011, **40**, 11192-11199; (b) M. Bühl, N. Sieffert, G. Wipff, *Dalton Trans.*, 2014, **43**, 11129-11137.
7   For other first-principles MD simulations of uranyl hydrate see: (a) R. Spezia, B. Siboulet, S. Abadie, R. Vuilleumier, P. Vitorge, *J. Phys. Chem. B*, 2011, **115**, 3560–3570; (b) R. J. Frick, T. S. HoferA. B. Pribil, B. R. Randolf, B. M. Rode, *J. Phys. Chem. A*, 2009, **113**, 12496–12503 (c) P. Nichols, E. J. Bylaska, G. K. Schenter, W. de Jong*, J. Chem. Phys.,* 2008, **128**, 124507. (d) D. Hagberg, G. Karlström, B. O. Roos, L. Gagliardi, *J. Am. Chem. Soc*., 2005, **127**, 14250-14256.
8   M. Bühl, N. Sieffert, A. Chaumont, G. Wipff, *Inorg. Chem.*, 2012, **51**, 1943-1952.
9   (a) G. M. Sheldrick, SHELXS-97, Göttingen (Germany), 1997; (b) G. M. Sheldrick, SHELXL-97, Göttingen (Germany), 1997.
10. R. Car, M. Parrinello, *Phys. Rev. Lett*., 1985, **55**, 2471-2474.
11 (a) A. D. Becke, *Phys. Rev. A*, 1988, **38**, 3098-3100; (b) C. Lee, W. Yang, R. G. Parr, *Phys. Rev. B*, 1988, **37**, 785-789.
12 U potential as generated in: M. Bühl, R. Diss, G. Wipff, *J. Am. Chem. Soc*., 2005, **127**, 13506-13507.

13 For pure liquid NH₃ (32 molecules in 11.229 Å box) this setup affords similar structural properties as in a previous study: A. D. Boese, A. Cgandra, J. M. L. Martin, D. Marx, *J. Chem. Phys*. 2003, **119**, 5965-5974.

14 We did not explore more sophisticated reaction coordinates such as coordination numbers. Using a simple distance as constraint could introduce some bias, but the concomitant error is probably smaller than that from the other approximations involved. For proton transfers, for instance, free energies within 4 kJ/mol had been obtained using either a simple X-H distance as coordinate or the coordination number about H, e.g. for water: (a) M. Sprik, *Chem. Phys,.* 2000, **258**, 139-150; or for histidine: (b) I. Ivanov, M. Klein, *J. Am. Chem. Soc. ,*2002, **124**, 13380-13381.

15 CPMD Versions 3.7.0 and 3.13.1, Copyright IBM Corp. 1990-2008, Copyright MPI für Festkörperforschung Stuttgart 1997 - 2001.

16 A. D. Becke *J. Chem. Phys.* 1993, **98**, 5648

17 (a) W. Küchle, M. Dolg, H. Stoll, H. Preuss,*J. Chem. Phys*., 1994, **100**, 7535-7542.

18 This small-core ECP has been shown to reproduce all-electron scalar relativistic results very well, see: S. O. Odoh, G. Schreckenbach, *J. Phys. Chem. A,* 2010, **114**, 1957-1963.

19 R. Krishnan, J. S. Binkley, R. Seeger, J. A. Pople, *J. Chem. Phys*., 1980, **72**, 650-654.

20 (a) B. Mennucci, J. Tomasi, *J. Chem. Phys.,* 1997, **106**, 5151-5158; (b) J. Tomasi, B. Mennucci, E. Cancés, *J. Mol. Struct. Theochem,* 1999, **464**, 211-226; (c) J. Tomasi, B. Mennucci, R. Cammi, *Chem. Rev.,* 2005, **105**, 2999-3093.

21 A. E. Reed, L. A. Curtiss, F. Weinhold, *Chem. Rev.,* 1988, **88**, 899-926.

22 M. J. Frisch, et al., Gaussian 09, Revision A.02, Gaussian, Inc., Wallingford CT, 2009 (see SI for full references).

23 L. J. Jouffret, S. V. Krivovichev, P. C. Burns, *Z. anorg. allg. Chem.* 2011, **637**, 1475–1480

24 S. V. Krivovichev, P. C. Burns, *Radiochemistry* 2004, **46,** 16–19.

25 G. A. Barclay, T. M. Sabine, T. C. Taylor, *Acta Cryst., Sect. B: Struct. Sci.,* 1965, **19**, 205–209.

26 A. Zalkin, L. K. Templeton, D. H. Templeton, *Acta Cryst., Sect. C* 1989, **45**, 810–811.

27 S. S. Malcic, L. M. Ljubica, Bull. B. Kidric. Inst. Nucl. Sci. 1961, **11**, 135–139.

28 Part of this discrepancy could also stem from the presence of the counteranions in the crystal, although in view of the similarity of the U-N distance with different coligands and counterions discussed above, this does not seem to be the overriding factor.

29 See e.g.: a) Rotzinger, F. P. *J. Phys. Chem. B,* 2005, **109**, 1510-1527; for assessment of DFT vs. ab initio methods for uranyl see e.g.: b) Rotzinger, F. P. *Chem. Eur. J.,* 2007**, 13**, 800 – 811; c) Wåhlin, P.; Danilo, C.; Vallet, V.; Réal, F.; Flament, J.-P.; Wahlgren, U. *J. Chem. Theory Comput*., 2008, **4**, 569-577.

30 For DFT computations see: (a) M. Bühl, N. Sieffert, A. Chaumont, Georges Wipff, *Inorg. Chem.*, 2011, **50**, 299–308; (b) M. Bühl, N. Sieffert, A. Chaumont, Georges Wipff, *Inorg. Chem.* 2012, **51**, 1943-1952; these findings are consistent with with experiments using electrospray ionization and ion-cyclotron resonance, where [UO₂(MeCN)$_n$]$^{2+}$ species (n = 1-4) readily take up water or acetonitrile, but the complex with n = 5 does not (i.e. water does not displace acetonitrile in the gas phase): (c) Van Stipdonk, M. J.; Chien, W.; Bulleigh, K.; Wu, Q.; Groenewold, G. S. *J. Phys. Chem. A* **2006,** *110,* 959-970; also gas-phase vibrational spectroscopy of [UO₂X(S)$_n$]$^{2+}$ species (X = anionic ligand) showed a more pronounced redshift of the ν₃ asymmetric UO₂ stretch (indicative of a stronger donor/acceptor) interaction for S = NH₃ than S = H₂O: (d) G. S. Groenewold, A. K. Gianotto, M. E. McIlwain, M. J. Van Stipdonk, M. Kullman, D. T. Moore, N. Polfer, J. Oomens, I. Infante, L. Visscher, B. Siboulet, W. A. de Jong, *J. Phys. Chem. A* **2008,** *112,* 508-521.

31 K. B. Wiberg, *Tetrahedron*, 1968, **24**, 1083.

32 M. Bühl, H. Kabrede, *Inorg. Chem.*, 2006, **45**, 3834-3836.